Elucidation of the electrochemical oxidation mechanism of the antioxidant sesamol on a glassy carbon electrode

by

R. Estévez Brito[a], J. M. Rodríguez Mellado[a,z] , P. Maldonado[b], M. Ruiz Montoya[c], A. Palma[c] and E. Morales[d]

[a]Departamento de Química Física y Termodinámica Aplicada
CeiA3, Campus Universitario Rabanales, IUIQFN, edificio Marie Curie
Universidad de Córdoba
E-14014-Córdoba (Spain)

[b]Institute of Chemical Research of Catalonia (ICIQ)
Av. Paisos Catalans 16
E-43007 Tarragona (Spain)

[c]Departamento de Ingeniería Química, Química Física y Química Orgánica
Facultad de Ciencias Experimentales
CeiA3, Campus de "El Carmen"
Universidad de Huelva
E-21071- Huelva (Spain)

[d]Departamento de Química y Ciencia de los Materiales
Facultad de Ciencias Experimentales
CeiA3, Campus de "El Carmen"
Universidad de Huelva
E-21071- Huelva (Spain)

[z]To whom correspondence should be addressed (e-mail: jmrodriguez@uco.es)

KEYWORDS: sesamol; 1,4-benzoquinone; electrode kinetics; antioxidants; glassy carbon electrode.

ABSTRACT

The dissociation constant of Sesamol (5- hydroxy-1,3-benzodioxol) was determined from the dependence of the UV-visible spectra with the medium acidity. A *pK* value of 10.1 ± 0.1, corresponding to the hydroxyl group, was obtained. The oxidation of sesamol was investigated on carbon electrodes using controlled-potential electrolysis, linear-sweep cyclic voltammetry and measurements at the foot of the first oxidation peak. Up to three oxidation peaks and one reduction peak were found. The dioxol ring of the dissociated sesamol undergoes a cleavage to give 3-substituted 1,4-benzoquinone, being the rate-determining step the second electron transfer. The formation of radicals in the ring cleavage explains in part the ability of sesamol to interact with reactive oxygen species (ROS).

INTRODUCTION

Seeking natural antioxidants is of increasing interest compared to "artificial" (synthetic) antioxidants used as food additives[1-3]. An antioxidant is a substance that may delay or prevent oxidation of an oxidizable substrate at low concentrations[4]. Primary and secondary antioxidants interact with radicals such as reactive oxygen species (ROS).

Direct electrochemical measurements are a rapid proof of the antioxidant capacity and, in consequence, they have been used for the determination of antioxidant activity[5,6]. To compare the antioxidant strength of phenolic acids, flavonoids, cinnamic acids etc, the oxidation potentials of cyclic voltammetric peaks have been used[7-10]. Low oxidation potentials are characteristic of high antioxidant activity, with good correlation with the technique of $DPPH^{\bullet}$ scavenging[11]. The substances showing activity in this assay are thermodynamically capable to react with agents that can reduce the $DPPH^{\bullet}$ radical.

Anodic oxidation of hydrogen peroxide on mercury electrodes has been used to determine the antioxidant character of phenolic compounds such as wines, strong alcohol beverages or beer[12-16]. The decrease in the oxidation current of hydrogen peroxide by adding the antioxidant is used to determine the antioxidant capacity. Suznkievic and coworkers[12] assessed that the anodic wave of H_2O_2 observed on mercury electrodes is due to the oxidation of Hg to Hg^{++} and the subsequent formation of a mixed complex with HO_2^- and OH^- ions, as previously reported by Kikuchi and Murayama[17]. A mechanism involving ROS generation was proposed[18], able to explain the decrease in the oxidation signal and assessing the scavenging character of the antioxidants

The scavenging capacity of an antioxidant is related to its oxidation mechanism. Moreover, the prooxidant capacity is linked to the oxidation potential. Thus, the aim of this work is to establish the electrochemical oxidation mechanism of sesamol to help in the understanding of its antioxidant activity.

Sesamol, 5- hydroxy-1,3-benzodioxol is a constituent of sesame oil with the structure shown below.

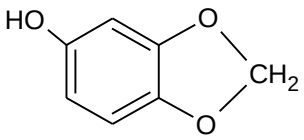

Sesamol

The antiphotooxidative activity of sesamol was attributed to the capture of singlet oxygen[19]. The antioxidant activity of sesamol[20-22], and for other natural products, was attributed to the phenolic group[20].

Experimental

All chemicals used in this work were Merck analytical grade reagents, with the exception of sesamol that was from Sigma-Aldrich, and were used without further purification.

Solutions containing 0.1 M in both acetic and phosphoric acids, for *pH*<8 and 0.05 M in both sodium carbonate and phosphoric acid at *pH*>8 were used as supporting electrolytes. The aqueous solutions were prepared using ultrapure water type I (resistivity 18.2 MΩ.cm at 298 K) obtained from an ultrapure water system Millipore. Ionic strength was adjusted to 0.3 M with solid KNO_3 and the *pH* was adjusted with solid NaOH. Stock solutions of sesamol were stored in the dark at 277 K to avoid decomposition.

UV measurements were made on a Perkin-Elmer Lambda 750S spectrophotometer with quartz cuvettes Hellma of path-length 1.0 cm. For the determination of the dissociation constant, the sesamol concentration was 0.1 mM, whereas the typical concentration for the electrochemical measurements was 1 mM.

All electrochemical measurements were made with an Autolab PGSTAT302 potentiostat using the software package GPES 4.9. A three-electrode cell (25 mL glass electrochemical cell) equipped with a Pt wire counter electrode, a BAS MF-2079 Ag/AgCl 3 M KCl reference electrode was employed. All tests were performed at 298 K.

For most electrochemical measurements, a glassy carbon electrode (IJCambria) with 7.5 mm^2 area was used as working electrode. The electrode was polished with a silicon carbide paper, followed by diamond (0.25 µm) slurry and alumina (0.3 and 0.05 µm) slurries. Residual polishing material was removed from the surface by sonication of the electrode in a water bath for 30 minutes after each polishing. The electrochemical pretreatment involved five cyclic voltammetry between +2 and –2 V on the untreated electrode in a saturated sodium chloride solution.

For the controlled-potential electrolysis, the working electrode was a high density graphite rod of 99.995% purity form Aldrich (CAS number 7782-42-5 C) protected with a silicone tube, which allow to use a cylinder with an area of 75.4 mm^2. The electrode was polished with a silicon carbide paper, followed by alumina (0.3 µm) slurry. Residual polishing material was removed from the surface by sonication of the electrode in a water bath for 20 minutes after each polishing. The counter electrode was a stainless steel rod. The electrolyses were made with samples of 5 mL of 1.2 mM sesamol and recording the charge along the experiment. To follow the course of the electrolysis, samples of 200 µL were taken after different amounts of charge were passed, added to 1.5 mL of purified water, and the corresponding UV-visible spectrum was recorded.

The compounds were analyzed using the solid phase microextraction (SPME) method. A SPME fiber, coated with 65 µm Polydimethylsiloxane/Diviylbenzene (PDMS/DVD) (Supelco, Bellefonte, PA) was inserted into a vial containing 3mL to electrolysis product solution for 30 min. The SPME fibers coating containing the products adsorbed was inserted

into the GC injection port at 230 ºC and remained for 3 min for desorption. After each sample injection, fibers were kept inside the SPME needle to prevent possible contamination and were conditioned with helium at 250 ºC for 10 min before reuse. The desorption of compounds was performed using a Shimadzu GC-2010 gas chromatography with a 30 m length and 0.25 mm diameter HP-5MS capillary column (J&W Scientific, Folsom, CA, USA) coupled with a Shimadzu mass spectrometer (Shimadzu corporation, Tokio, Japón) operating in EI mode at 70 eV. The transfer line between the GC and MS instruments was kept at 280°C.The gas chromatograph system was equipped with a split/splitless injection port operating in Splitless mode. The oven temperature program was: initial temperature 35°C (5 min), increased to 220°C at 15°C/min, then increased to 270ºC at 50ºC/min, and held for 2min. Helium (99.999%) was used as the carrier gas, at a flow rate of 1 mL/min. The mass spectrometer was operated in the full scan (scan) in the mass range m/z = 33-350. Identification of compounds was achieved comparing the mass spectra with the data system library (NIST 08). When necessary, derivatization was made using trifluoroacetic anhydride[23].

Results and discussion

In order to obtain the dissociation constant of sesamol, UV-visible absorption spectra were recorded as a function of *pH*. The curves presented three main bands in the entire *pH* interval, with maxima at 230-240, 292 and 311 nm, having two isosbestic points at 269.5 and 301 nm, as can be seen in Figure 1. Below *pH* 7 and above *pH* 11, the spectra were unchanged. The dependence of the spectra with the medium acidity shown in Figure 1 indicates that sesamol is involved in an acid-base equilibrium. The corresponding *pK* was obtained from the absorbance measured at constant wavelength by plotting $\log[(A-A_1)/(A_2-A)]$ *vs. pH*, where A_1 and A_2 are the constant absorbance values found at *pH* below and above the variation of absorbance, respectively. The *pK* value so obtained was 10.1 ± 0.1, corresponding to the hydroxyl group and in agreement with that calculated using ACD/Labs software, and also

agrees with that obtained from the plot of the oxidation peak potential of the main peak vs. pH, as will be shown below.

– – – FIGURE 1 – – –

In linear-sweep cyclic voltammetry (LSCV) on a glassy carbon, sesamol exhibits up to three oxidation peaks and one reduction peak depending on whether one or two successive cycles are recorded. As it is shown in Figure 2, the first cycle of the voltammogram shows two oxidation peaks, named *Peak 1* and *Peak 2* attending the higher oxidation potential at which they appear, and one reduction peak I, named *Peak 3'*, appearing at less positive potentials. In the second cycle, in addition to peaks 1 and 2, a new oxidation peak, named *Peak 3*, appears at potentials slightly more positive than peak 3'. Peaks 1 and 2 appeared in the entire *pH* range studied (1-12.5) whereas peaks 3 and 3' were not observed above *pH* 10.

– – – FIGURE 2 – – –

Two scans of cyclic voltammograms were recorded in the sequence oxidation-reduction, switching the scans at a potential localized after peak 1 and before the starting of peak 2. Under such conditions, the voltammogram corresponding to the 3-3' system in the second scan was identical to that obtained when the scan was switched after peak 2, as in Figure 2. Therefore, it can be concluded that the redox system formed by peaks 3 and 3' is related to the process occurring at the potentials of peak 1 and not to those taking place at the potentials of peak 2.

The species that is oxidized at the potentials of peak 3 must be different from sesamol and must be related with the oxidation product obtained at the potentials of peak 1. To check this assumption, a constant potential above peak 1 during a given time, t_d was applied. After this deposition time, a voltammogram was recorded in the potential window corresponding to the 3-3' system, starting with the reduction scan followed by the oxidation scan. In another set of experiments, the same voltammogram was obtained but in the oxidation-reduction sequence.

This was made by varying t_d as shown in Figure 3. The two sets of experiments show similar results: the intensities of the peaks remain constant at $t_d \geq 20$ s, though the ratio between the intensities of 3' and 3 peaks is close to unity in the reduction-oxidation scan sequence, and slightly lower in the reverse scan sequence.

– – – FIGURE 3 – – –

Let one consider the structure of sesamol. The more plausible oxidation reaction occurring at the potentials of peak 1 must involve cleavage of the five-membered ring to give either a 1,3-benzoquinone or a 1,4-benzoquinone. But 1,3-benzoquinone does not exist, because the structure would be nonplanar and highly strained, and the proposed overall reaction for peak 1 is:

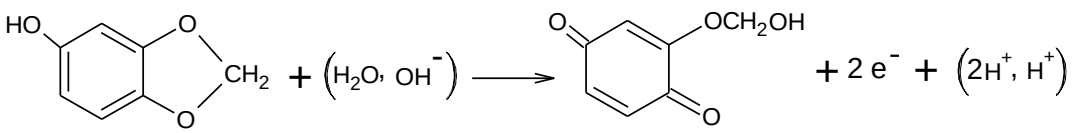

Scheme I

The substituted 1,4-benzoquinone formed remains in the proximity of the electrode and can be reduced in the reverse scan at the potentials corresponding to the 3' peak and the resulting 1,4-dihydrobenzoquinone is oxidized in the next cycle at the potentials corresponding to the 3 peak, less negative than the sesamol oxidation potential:

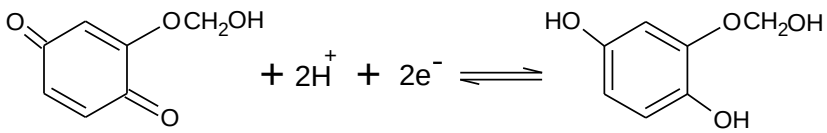

Scheme II

Evidences for the above scheme are inferred. First, the dependence of the peak potentials with the *pH* corresponding to the 3-3' system is compatible with the redox process corresponding to scheme 3. The 3-3' system was recorded at different *pH* values with $t_d = 20$ s.

As it can be seen in Figure 4, the peak potentials of both the oxidation and reduction peak shift around –0.059 V per *pH* unit, this corresponds to the intervention of two H^+ ions for a two-electron process, as in the case of 1,4-benzoquinone[24].

– – – FIGURE 4 – – –

The number of electrons taking part in the process occurring at the potentials of peak 1 can be obtained by comparison of the voltammogram with the signal obtained for 1,4-dihydrobenzoquinone. This is shown in Figures 5A and 5B. As it can be seen, the oxidation peaks of sesamol and 1,4- dihydrobenzoquinone are very similar.

– – – FIGURE 5 – – –

Nevertheless, the peak intensity in voltammetry depends on the mechanism of the redox process and cannot be used for comparison unless the mechanisms of the compared processes were the same.

Convolution voltammetry[25-30] was used to analyse the oxidation scans of the voltammograms by computing the integral

$$J = \pi^{-1/2} \int_0^t \frac{I(\nu)}{(t-\nu)^{1/2}} d\nu \qquad (1)$$

where I is the actual current, J is the convoluted current, v is an integration variable, and t is related to the potential through the scan rate. S-shaped curves are obtained with limiting values, J_L, independent of the mechanism of the electrochemical reaction:

$$J_L = nFAD^{1/2}c_0 \qquad (2)$$

where n is the number of electrons involved in the process, A is the electrode area, and D and c_0 are the diffusion coefficient and the bulk reactant concentration, respectively.

Figure 5B shows that the limiting currents of the convoluted voltammograms corresponding to sesamol and 1,4- dihydrobenzoquinone are very similar; the slight difference

being due to the difference of diffusion coefficients, In conclusion, two-electrons are involved in the process occurring at the potentials of peak 1.

– – – FIGURE 5 – – –

To strengthen the above conclusions, bulk electrolyses were made at a potential placed after peak 1 and before peak 2 and the color of the solution changed gradually from practically colorless to orange. Figure 6 shows the spectra obtained along the electrolysis. As can be seen, the UV-visible spectrum at the end of the electrolysis is very different of the spectrum of sesamol, showing the three bands characteristic of the p-benzoquinone ring[31], centered at 380 nm, 290 nm and 250 nm, in this case.

– – – FIGURE 6 – – –

The number of electrons involved in the oxidation process was obtained from the slope of the plot of the charge vs. mol of oxidized sesamol. The plot shown in figure 6 confirms the two-electron nature of the peak 1. Since two faradays per mol of sesamol are needed to obtain the product, an electrolysis was made passing the charge corresponding to the amount of sesamol in the cell. The solution containing the oxidation product was analyzed with solid-phase micro-extraction and GC-MS (see experimental) and after several attempts changing the experimental conditions it was concluded that the boiling point of the product is higher than the maximum operative temperature of the chromatograph. So, a derivatization was made using trifluoroacetic anhydride and a fluorinated derivative of (hydroxymethoxy)-1,4-benzoquinone was identified.

Figure 5A also reveals that the peak potential of the oxidation peak of 1,4-dihydrobenzoquinone is lower than the peak potential of peak 1, that is, the 1,4-dihydrobenzoquinone is oxidized at lower potentials than sesamol. In addition, the redox process of the 3-3’ system is very similar to that corresponding to 1,4- dihydrobenzoquinone.

The lower oxidation peak potentials found for the 3-3' system can be attributed to the presence of the substituent at position 3. The hydroxymethoxy group is strongly activating due to the resonance effect of the oxygen atom bonded to the ring, and the negative charge originated on the ring facilitates the oxidation.

Diagnostic criteria for the electrochemical processes can be established using logarithmic analyses based on the equation[25-30]:

$E = E_{1/2} + b \ln[f(I, J)]$ (3)

where f(I, J), $E_{1/2}$ and b depend on the actual mechanism of the electrochemical reaction as is shown in Table 1.

– – – TABLE 1 – – –

The direct scans of the voltammograms were analyzed using the f(I, J) corresponding to a reversible process and the result is given in Figure 5D. The logarithmic analyses of peak 3 are very similar to those corresponding to the oxidation peak of 1,4-benzoquinone.

All these facts indicate that the mechanism of the process shown in scheme III must be very similar, if not the same, as the oxidation-reduction of 1,4-benzoquinone.

The process occurring at the potentials corresponding to peak 1 is, evidently, irreversible. Nevertheless, the electron transfers can be reversible, since the ring cleavage step can be placed after the electron transfers. The application of equation 3 to the convoluted voltammograms, using the f(I, J) corresponding to an irreversible/EC process, gives b values of 0.045 V (at 298 K) at $pH<pK_a$; this indicates that the second electron transfer must be the rate-determinig step, r.d.s., of the oxidation process[32-34]. In addition, the $E_{1/2}$ values were independent of both the scan rate and the concentration of sesamol; the J_L values were independent of the scan rate and proportional to the sesamol concentration. These dependencies are required for the application of the diagnostic criteria.

The above conclusions were also confirmed using differential pulse voltammetry, DPV. The analysis of the DP voltammograms was performed by using the following equation corresponding to first-order processes[35]:

$$I = 4I_P \frac{L}{(1+L)^2} \qquad (4)$$

where $L = \exp[-(E-E_P)/b]$, I_P and E_P being the peak intensity and peak potential, respectively, and b is a parameter which has the same value and meaning as the slope of the convolution logarithmic analysis[35,36].

Equation 4 corresponds to a symmetrical peak where the area of the curve is proportional to the concentration of depolarizer (and also proportional to $b \cdot I_P$) and to the overall number of electrons involved in the electrochemical process. The DPV peaks of sesamol were well described by equation 4 until the peak potential and even to potentials above this value. Nevertheless, the proximity of the background discharge causes a distortion for potentials more positive than the peak potential and the curve is distorted. Thus, the b parameter was obtained from the fitting of the experimental results to equation 4 at potentials below E_P. At $pH < pK_a$ the b values so obtained were of 41-43 mV, corresponding to a two-electron process in which the rate-determining step, r.d.s., is the second electron transfer[35,36]. At $pH > pK_a$ the b values were of 32-33 mV, corresponding to a process involving two reversible electron transfer.

The linearity of the convolution logarithmic analyses is poor at high *pH* values (i.e. at $pH > pK_a$). For this reason, the *i*-*E* curves were analyzed at potentials corresponding to the foot of the voltammetric curves, where the contribution of the transport is minimal and it is possible to obtain the Tafel curves and the electrochemical reaction orders.

The *E* vs. log *i* plots were linear at such range of potentials, having slopes (at 298 K) of 43-45 mV, at *pH* values lower than the pK_a, and close to 32 mV at higher *pH* values. In the first case, the Tafel slopes agree with the convolution logarithmic analysis slopes, which confirms

that the second electron transfer must be the rate-determinig step, r.d.s., of the oxidation process at these *pH* values. At $pH>pK_a$ the Tafel slope is compatible with two reversible electron transfers. Since the overall process is irreversible, the mechanism occurring at these *pH* values must be of E_rE_rC type, i.e., the r.d.s. must be a chemical reaction placed after two reversible electron transfers. This reaction must be the ring cleavage.

The electrochemical reaction orders can be obtained from the dependence of the Tafel plots on the concentration of reactants, in this case on the concentration of sesamol and H^+ ion. These orders were unity for sesamol, irrespective of the *pH*, and –1.1 and 0 for *pH* values lower and higher of pK_a, respectively.

Based upon all the results and conclusions, the following reaction scheme is proposed for the potentials of peak 1:

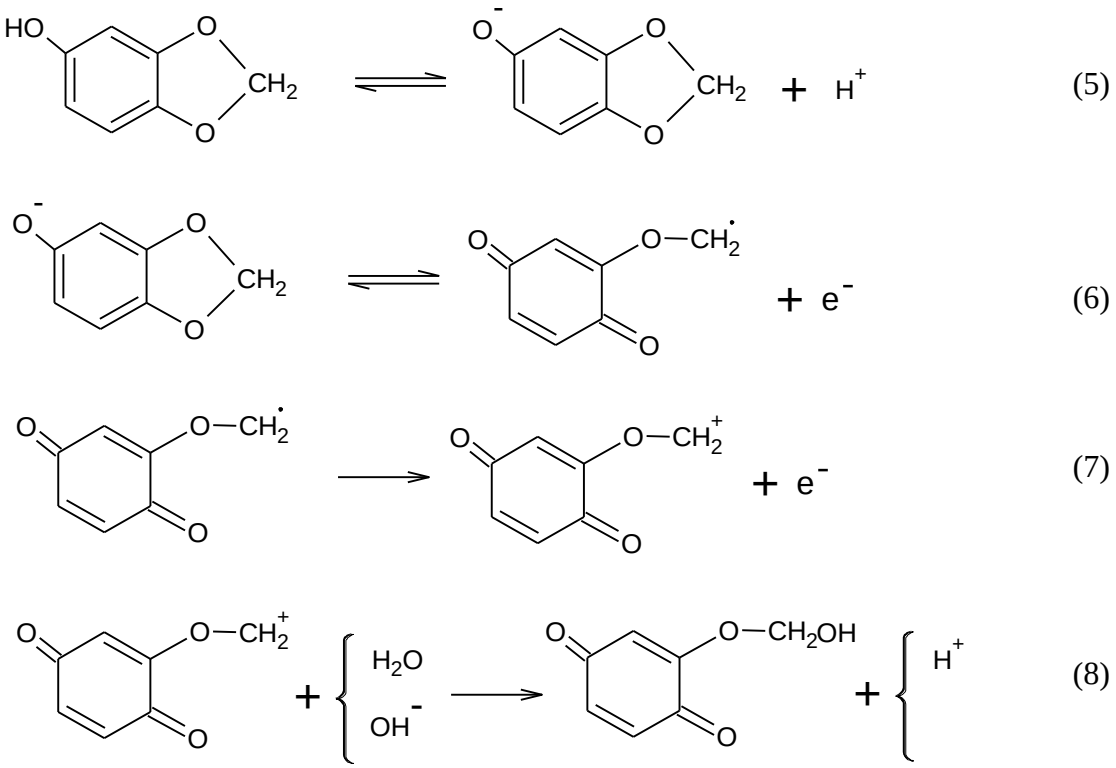

In this scheme, reaction (5) occurs only at $pH<10.1$ (the dissociation pK_a) and is absent above this *pH* value.

Below *pH* 10.1, reaction (7) is the r.d.s. whereas in very basic media the rate of the process is given by reaction (8). The i-E-t relationships for these processes can be obtained by using the convective diffusion approximation and the steady-state conditions. Moreover, the differential equations of the Nernst diffusion-layer approximation can be solved by the method of dimensionless variables applied as shown in the literature[37-42]. Using this approximation, the following equation can be obtained:

$$i = 2FK_5K_6k_7K'c_H^{-1}c_S \exp\left[\frac{(1+\beta)FE}{RT}\right] \qquad (9)$$

where K_5 and K_6 are the equilibrium constants of reactions (5) and (6), k_7 is the rate constant of rection 7 at zero potential, c_H and c_S are the concentrations of H^+ ion and sesamol, respectively, and *K*'=exp[(1+β)F$\triangle\phi_{ref}$/RT], β the symmetry factor and $\triangle\phi_{ref}$ the potential of the reference electrode.

The electrochemical reaction orders derived from equation (9) are –1 and 1, for the H^+ ion and sesamol, respectively, and the Tafel slope is 2.303RT/(1+β)F, that is, 0.039 mV at 298 K (assuming β=0.5). All the experimental results agree with these predictions.

Above *pH* = 10.1, the equation to be fulfilled at the potentials of the foot of the peak is:

$$i = 2FK_6K_7k_8K'c_S \exp\left[\frac{2FE}{RT}\right] \qquad (10)$$

where the symbols have the abovementioned meanings and K'=exp[(2F$\triangle\phi_{ref}$/RT].

The electrochemical reaction orders derived from equation 10 are 0 and 1, for H^+ ion and sesamol, respectively, and the Tafel slope is 2.303RT/2F, that is, 0.029 mV at 298 K. Again, all the experimental results agree with these predictions.

The analysis of peak 2 is difficult due to its proximity to the background discharge. As it can be seen in Figure 4, the peak potentials of this peak do not shift with the *pH* except at

very high *pH* values. Moreover, below *pH* 9, the convoluted limiting current of peak 2 is the same as that corresponding to peak 1, but increases to the double at *pH*>10. This implies that the process occurring in acidic and neutral media is two-electron whereas it is a four-electron, in very basic solutions.

The reactant for the oxidation process occurring at these potentials must be the substituted 1,4-benzoquinone obtained in the preceding oxidation. Since the peak potential is not *pH*-dependent, the H^+ or OH^- ions do not take part in the process, at least prior or in the r.d.s. Thus, it could be postulated that the substituted 1,4-benzoquinone is hydrolyzed by a water molecule to yield hydrated formaldehyde and 3-hydroxy-1,4-benzoquinone, which is subsequently oxidized to the corresponding peroxide with the participation of another water molecule. In very basic solutions, the hydrolysis is made by the OH^- ions, this explaining the shifting of the peak potentials, and the oxidation progresses beyond the peroxide.

The antioxidant activity of sesamol measured by means of the DPPH• test and cyclic voltammetry is medium-high[11]. The radical scavenging versus ROS measured by differential pulse voltammetry using the H_2O_2 oxidation was medium-low[18]. Such antioxidant character of sesamol can be attributed to the relative lability of the five-membered ring to give a quinone. The formation of this molecule is responsible for the antioxidant activity of sesamol, rather than the presence of the phenolic group in the molecule postulated in the literature[20]. In addition, the formation of radicals in the ring cleavage can explain in part the ability of sesamol to interact with ROS.

Acknowledgements

Financial support from Junta de Andalucía (Research Groups FQM-0198, RNM-371 and FQM-0348) is gratefully acknowledged.

References

1. K. Dastmalchi, H. J. Damien Dorman, Kosar M., R. Hiltunen, *Food Sci. Technol.* **40**, 239 (2007).

2. M. Carocho, I.C.F.R. Ferreira, *Food Sci. Technol.* **51**, 15 (2013).

3. S. Maqsood, S. Benjakul, F. Shahidi, Crit. Rev. Food Sci. Nutrition, **53**, 162 (2013)

4. J.M. Gutteridge and B. Halliwell, *Ann. N. Y. Acad. Sci.*, **899**, 136 (2000).

5. P. A. Kilmartin, Z. Honglei and A. L. Waterhouse, *Am. J. Enol. Vitic.*, **53**, 294 (2002).

6. P. A. Kilmartin, H. Zou and H.Waterhouse, *J. Agric. Food Chem.*, **49**, 1957 (2001).

7. R. Bortolomeazzi, N. Sebastianutto, R. Toniolo, and A. Pizzariello, *Food Chem.*, **100**, 1481 (2007).

8. M. A. Samra, V. S. Chedea, A. Economou, A. Calokerinos, and P. Kefalas, *Food Chem.*, **125**, 622 (2011).

9. K. E. Yakovleva, S. A. Kurzeev, E. V. Stepanova, T. V. Fedorova, B. A. Kuznetsov, and O. V. Koroleva, *App. Biochem. Microbiol.*, **43**, 661 (2007).

10. S. Chevion, M. A. Roberts, and M. Chevion, *Free Radical Biol. Med.*, **28**, 860 (2000).

11. J. F. Arteaga, M. Ruiz Montoya, A. Palma, G. Alonso Garrido, S. Pintado and J. M. Rodríguez Mellado, *Molecules*, **17**, 5126 (2012).

12. D. Ž. Sužnjević, F. T. Pastor and S. Ž. Gorjanović, *Talanta*, **85**, 1398 (2011).

13. S. Ž. Gorjanović, M. M. Novaković, N. I. Potkonjak, I. Leskošek-Čukalović and D. Ž. Sužnjević, *J. Agric. Food Chem.*, **58**, 744 (2010).

14. S. Ž. Gorjanović, M. M. Novaković, N. I. Potkonjak and D. Ž. Sužnjević, *J. Agric. Food Chem.*, **58**, 4626 (2010).

15. S. Ž. Gorjanović, M. M. Novaković, P. V. Vikosavijević, F. T. Pastor, V. V. Tešević and D. Ž. Sužnjević, *J. Agric. Food Chem.*, **58**, 8400 (2010).

16. M. M. Novaković, S. M. Stevanović, S. Ž. Gorjanović, P. M. Jovanovic, V. V. Tešević, M. A. Janković and D. Ž. Sužnjević, *J. Food Sci.*, **76**, C663 (2011).

17. Kikuchi, K; Murayama, T., *Bull. Chem. Soc. Japan* **1976**, 49, 1554-1556

18. A. Palma, M. Ruiz Montoya, J. F. Arteaga and J. M. Rodríguez Mellado, *J. Agric. Food Chem.* **62**, 582 (2014)

19. J. Y. Kim, D. S. Choi, M. Y. Jung, *J. Agric. Food Chem.* **51**, 3460 (2003).

20. R. Joshi, M. S. Kumar, K. Satyamoorthy, M. K. Unnikrisnan, T. Mukherjee, *J. Agric. Food Chem.* **53**, 2696 (2005).

21. S. W. Lee, M. K. Jeung, M. H. Park, S. Y. Lee, J. Lee, *Food Chem.* **118**, 681 (2010).

22. H. Yoshida, S. Takagi, *J. Sci. Food Agric.* **79**, 220 (1999).

23. G. Fauler, t H. J. Leis, J. Schalamon, W. Muntean and H. Gleispach *J. Mass Spectrometry*, **31**, 655 (1996)

24. P. S. Guin, S. Das, P. C. Mandal, *Int. J. Electrochem*. **2011**, 816202 (2011)

25. C.P. Andrieux, L. Nadjo, J.M. Savéant, *J. Electroanal. Chem*., **26**, 147 (1970).

26. J.C Imbeaux, J.M. Savéant, *J. Electroanal. Chem*. **44**, 169 (1973).

27. J.M. Savéant, D. Tessier, *J. Electroanal. Chem.*, **61**, 251 (1975).

28 J.M. Savéant, D. Tessier, *J. Electroanal. Chem.*, **77**, **225** (1977).

29. D.B. Oldham, *Anal. Chem*., **44**, 196 (1972); *J. Chem. Soc. Faraday Trans. I*, **82**, 1099 (1986)

30. G.D. Zoski, D.B.Oldham, P.J. Mahon, T.L.E. Menderson, A.M. Bond, *J. Electroanal. Chem.*, **297**, 1 (1991)

31. NIST Standard reference data, U.S. Secretary of Commerce, Vol. 69 (2011), http://webbook.nist.gov/cgi/cbook.cgi?ID=C106514&Mask=400

32. R. S. Nicholson and I. Shain, *Anal. Chem*. **36**, 706 (1964)

33. J. M. Rodríguez Mellado, *Ann. Chim.* **83**, 279 (1993).

34. M. Ruiz Montoya, J. M. Rodríguez Mellado, *J. Electroanal. Chem.*. **370**, 183 (1994).

35. J. M. Rodríguez Mellado, M. Blázquez, M. Domínguez and J. J. Ruiz, *J. Electroanal. Chem.* **195**, 263 (1985).

36. J. M. Rodríguez Mellado, M. Blázquez and M. Domínguez, *J. Electroanal. Chem.*, **201**, 237 (1986).

37. P. Andrieux, L. Nadjo and J. M. Savéant, *J. Electroanal. Chem.* **42**, 223 (1973).

38. L. Nadjo and J.M. Savéant, *J. Electroanal. Chem*, **137**, 149 (1982).

39. J. E. Cosano, A. M. Heras, L. Camacho, J. L. Avila and J. M. Rodríguez Mellado, *J. Electroanal. Chem.* **195**, 321 (1985).

40. E. Muñoz, L. Camacho, J. L. Avila, A. M. Heras and J. J. Ruiz, *Bull. Soc. Chim. Belg*. **96**, 255 (1987).

41. A. M. Heras, E. Muñoz, J. L. Avila, and L. Camacho, *Electrochim. Acta*, **32**, 1495 (1987).

42. R. Ortiz, M. J. Higuera, R. Marín Galvín and J. M. Rodríguez Mellado, *J. Electrochem. Soc.* **148**, E419 (2001).

Table headings

Table 1. Values of m (antioxidant concentrations in $mM \cdot L^{-1}$), ARP and oxidation potentials vs. Ag/AgCl/KCl (3M) electrode for the antioxidants studied.

Figure Captions

Figure 1. A) UV-visible spectra of $1 \cdot 10^{-4}$ M sesamol solutions at different pH values. B) Plot of the absorbance measured at two wavelengths vs. pH. C) Plot of $\log[(A-A_{min})/(A_{max}-A)]$ vs pH.

Figure 2. Linear-sweep cyclic voltammograms of $1 \cdot 10^{-5}$ M sesamol at a scan rate of 0.1 $V \cdot s^{-1}$ and pH = 1.74

Figure 3. Linear-sweep cyclic voltammograms of the 3-3' system of $1 \cdot 10^{-5}$ M sesamol after deposition at 0.900 V and deposition times (in seconds) given in the figure. pH = 1.80. v=0.1 $V \cdot s^{-1}$. Up: starting potential 0.600 V. Down: starting potential –0.200 V. Arrows indicate the initial direction of the scan.

Figure 4. Dependencies of the peak potentials of the voltammetric peaks on the solution pH for $1 \cdot 10^{-5}$ M sesamol. v=0.1 $V \cdot s^{-1}$.

Figure 5. A) Linear-sweep cyclic voltammograms of $1 \cdot 10^{-5}$ M sesamol and $1 \cdot 10^{-5}$ M 1,4-dihydrobenzoquinone at pH 2.5 and v=0.1 $V \cdot s^{-1}$. B) Convoluted voltammograms of the oxidation peaks C) Linear-sweep cyclic voltammograms of the 3-3'system of $1 \cdot 10^{-5}$ M sesamol after 60 s deposition at 0.900 V and $1 \cdot 10^{-5}$ M 1,4-dihydrobenzoquinone. D) Logarithmic analyses of the convoluted oxidation peaks of fig. D.

Figure 6. UV-visible spectra of the electrolyzed solution at different times (shown in the figure).

Inset: plot of the charge in microfaradays versus the electrolyzed amount of sesamol.

Process	f(I, J)	$E_{1/2}$	b
Reversible (E_r)	$\frac{J}{J_L - J}$	E_0'	$\frac{RT}{nF}$
Irreversible (E_i)	$\frac{I}{J_L - J}$	$E_0' + \frac{RT}{\alpha nF} \ln \frac{k_f^0}{D^{1/2}}$	$\frac{RT}{\alpha nF}$
Chemical reaction following an E_r process E_rC_i	$\frac{I}{J_L - J}$	$E_0' + \frac{RT}{2nF} \ln k$	$\frac{RT}{nF}$

Table 1

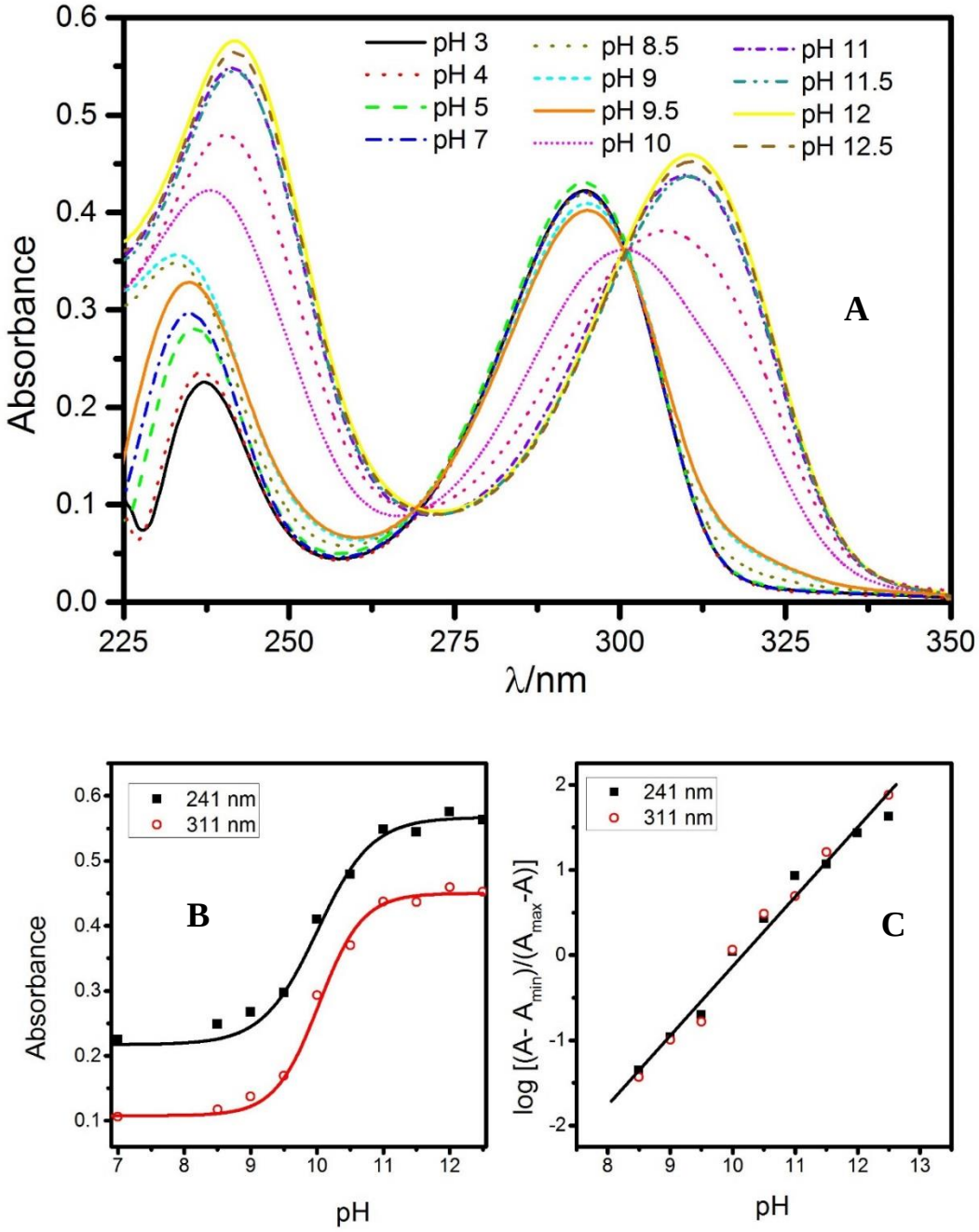
pH 3
pH 4
pH 5
pH 7
pH 8.5
pH 9
pH 9.5
pH 10
pH 11
pH 11.5
pH 12
pH 12.5
Absorbance
λ/nm
A
241 nm
311 nm
B
Absorbance
pH
241 nm
311 nm
C
log [(A- A_min)/(A_max-A)]
pH

Figure 1

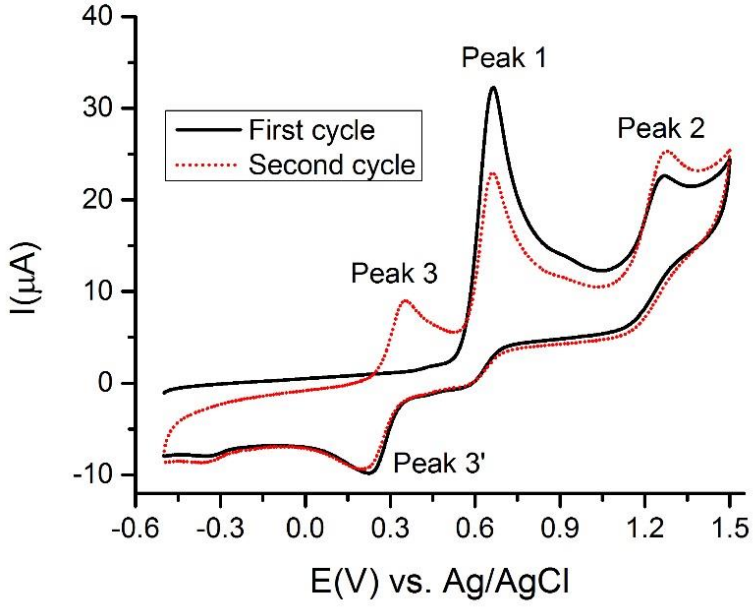
40
30
20
10
0
-10
I(μA)
Peak 1
Peak 2
Peak 3
Peak 3'
First cycle
Second cycle
-0.6
-0.3
0.0
0.3
0.6
0.9
1.2
1.5
E(V) vs. Ag/AgCl

Figure 2

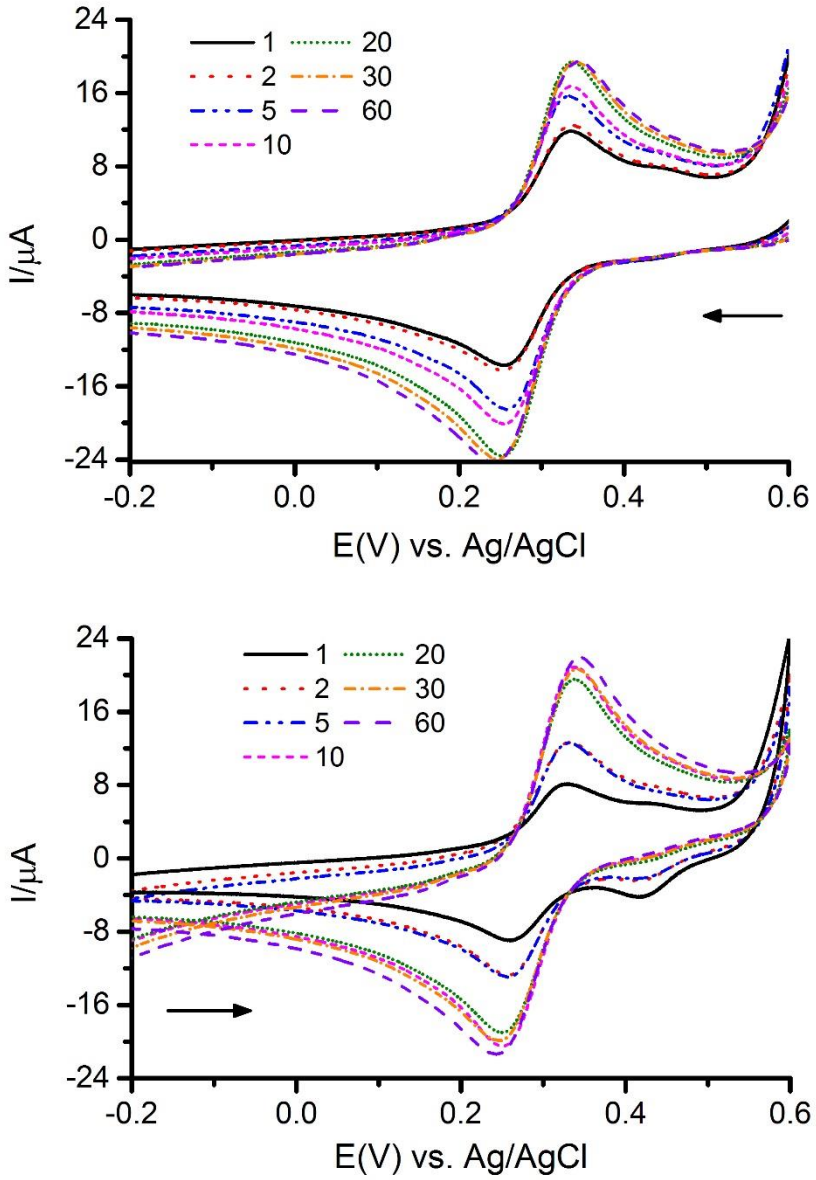

Figure 3

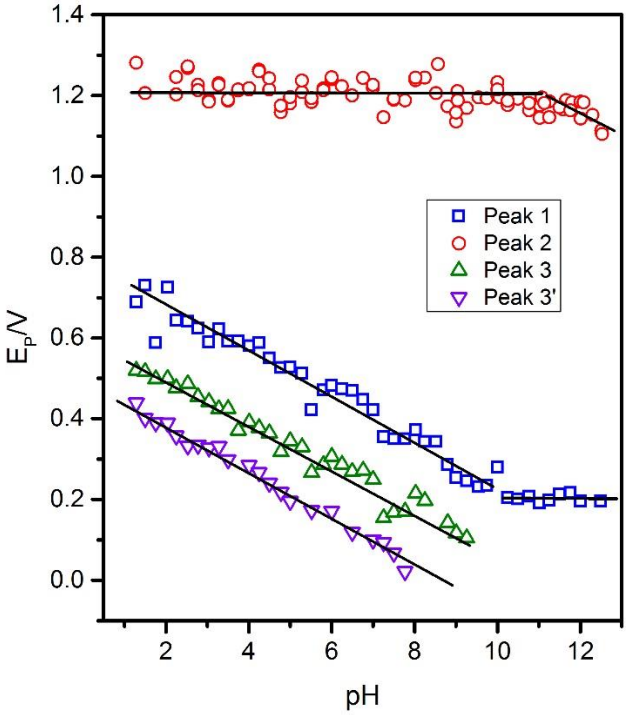

Figure 4

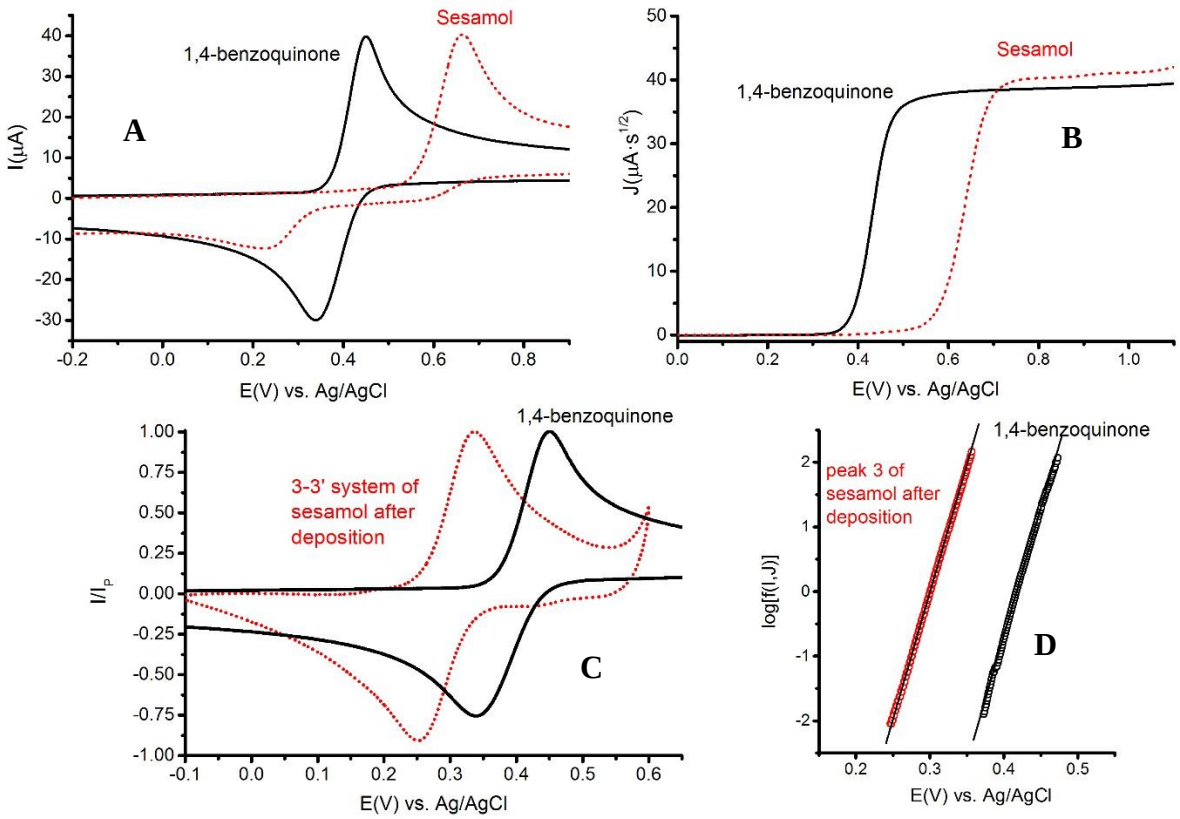
A
Sesamol
1,4-benzoquinone
I(μA)
E(V) vs. Ag/AgCl
B
Sesamol
1,4-benzoquinone
J(μA·s^1/2)
E(V) vs. Ag/AgCl
C
1,4-benzoquinone
3-3' system of sesamol after deposition
I/I_P
E(V) vs. Ag/AgCl
D
1,4-benzoquinone
peak 3 of sesamol after deposition
log[f(I,J)]
E(V) vs. Ag/AgCl

Figure 5

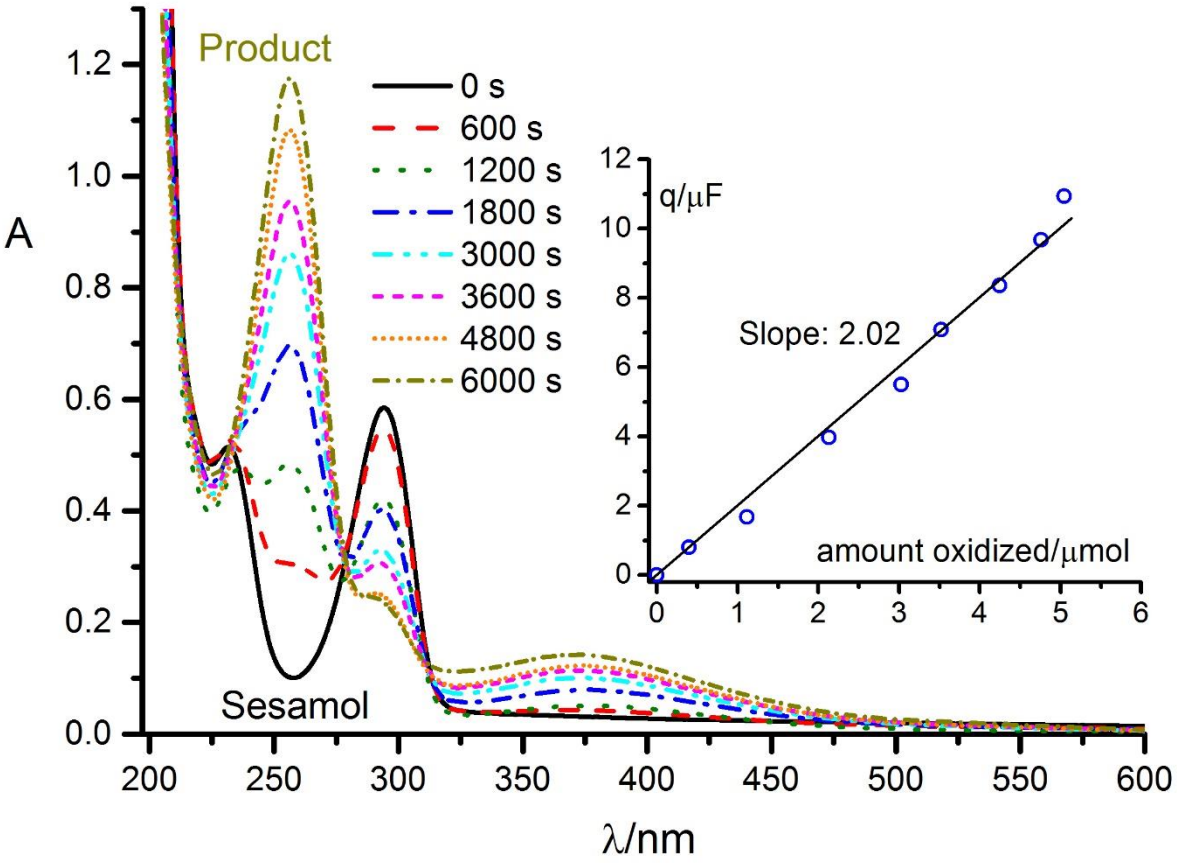
Product
0 s
600 s
1200 s
1800 s
3000 s
3600 s
4800 s
6000 s
Sesamol
A
λ/nm
q/μF
Slope: 2.02
amount oxidized/μmol

Figure 6